EXPERIMENTAL AND MODEL-COMPUTED AREA-AVERAGED VERTICAL PROFILES OF WIND SPEED FOR EVALUATION OF MESOSCALE URBAN CANOPY SCHEMES

Michael Brown[1], Suhas Pol[1], William Coirier[6], Sura Kim[6], Alan Huber[3], Matt Nelson[1], Petra Klein[5], Matt Freeman[4], and Akshay Gowardhan[1,2]

[1]Los Alamos National Laboratory, [2]University of Utah, [3]NOAA/USEPA
[4]Lockheed-Martin/USEPA, [5]Oklahoma University, [6]CFD Research Corporation

1. INTRODUCTION

Numerous urban canopy schemes have recently been developed for mesoscale models in order to approximate the drag and turbulent production effects of a city on the air flow. However, little data exists by which to evaluate the efficacy of the schemes since "area-averaged" wind measurements in cities are difficult to obtain owing to the large number of wind sensors required to obtain a reasonable statistical sample. In this study, we have computed quasi-area-averaged vertical profiles of wind speed for several recent field and wind-tunnel experiments where a relatively large number of wind measurements were taken. In addition, we have derived area-averaged profiles using numerical model-computed mean wind fields from simulations performed in several cities. These computational fluid dynamics codes have the advantage of producing a dense array of "measurements" which can be used to obtain a more statistically-significant area average.

In this paper, we will describe the experimental data we have used and show vertical profiles of area-averaged wind speed for several realistic and idealized multi-building array configurations. We will then discuss the use of numerical models for creating "synthetic" data and compare area-averaged model-computed results for several cities. We will finish by discussing how the area-averaged wind speed may change as a function of plan area density (λ_p), frontal area density (λ_f), standard deviation of building heights (σ_h), and other relevant parameters.

Corresponding author address: Michael Brown, LANL, Group D-3, MS F607, Los Alamos, NM 87545.
E-mail – mbrown@lanl.gov

2. BACKGROUND

Groups of buildings, on average, act to slow down the wind through drag and obstacle deflection of the flow, regions of reverse flow in building-induced circulations, and zones of calm winds between buildings. A number of research groups have been adding urban canopy parameterizations to mesoscale models in order to approximate the sub-grid effects of buildings on the mean flow and turbulent kinetic energy fields (e.g., Sorbjan and Uliasz, 1982; Brown and Williams, 1998; Ca et al., 1999; Urano et al., 1999; Martilli et al., 2002; Otte et al., 2004; Holt and Shi, 2004; Chin et al., 2005).

These parameterizations have generally been implemented with a sink term added to the momentum equations and with a production term added to the turbulent kinetic energy equation (see reviews by Brown (1998) and Masson (2005)). The drag term, usually a function of the frontal area density of buildings ($\lambda_f(z)$), results in a mesoscale-model-produced wind speed profile that resembles the Cionco (1972) vegetative canopy profile:

$$u(z) = u_H \exp\left(a\left(\frac{z}{H} - 1\right)\right), \qquad (1)$$

where H is canopy height, U_H is the wind at canopy height, and a is an attenuation coefficient proportional to the porosity of the canopy.

The wind field produced by the mesoscale model can be thought of as representing the average wind over the computational grid cell (generally on the order of 1 km in horizontal dimension). Since winds in urban areas can be

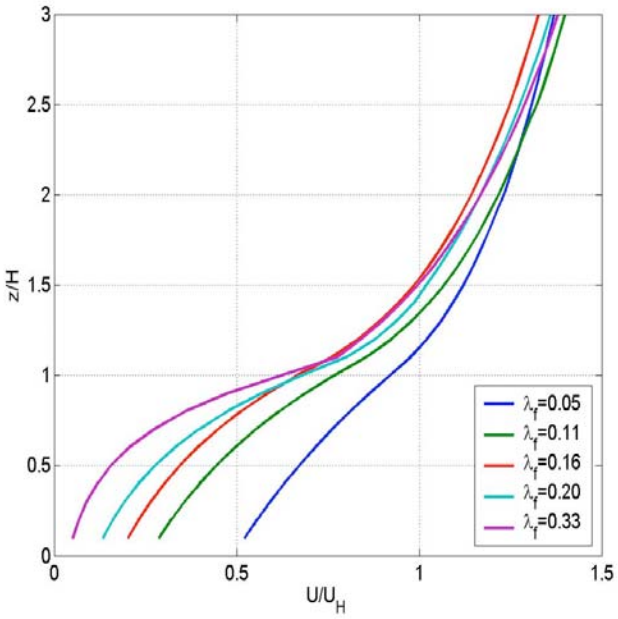

Figure 1. Examples of area-averaged urban canopy profiles with different frontal area densities using the blended formula of Macdonald (2000).

extremely complex, with flow on one side of the street opposite to that on the other, a single vertical profile of wind speed measurements from a tower, for example, will not be representative of the mesoscale model grid cell value.

For evaluating winds produced by mesoscale models, a large number of wind sensors at nearly the same height distributed horizontally over at least a several block area is required to obtain a "measurement" at a particular height. If multiple horizontal planes of instrumentation are available, then a vertical profile of these "area-averaged" measurements can be used to evaluate the mesoscale model urban canopy parameterizations.

Area-averaged wind speed profiles have been obtained from several laboratory reduced-scale experiments. Macdonald (2000) performed numerous building-array flow experiments in a flume and obtained quasi-area-averaged profiles for staggered and aligned cubical building arrays for a wide range of packing densities. Macdonald found that the Cionco exponential profile matched the data well for a frontal area density (λ_f) less than 0.3, but a linearly-varying profile fit the data better for tightly-packed staggered building arrays (note that this latter result holds for the area-average U component of velocity, not necessarily wind speed). Macdonald also found that the attenuation coefficient a = 9.6 λ_f for aligned and staggered arrays of cubes and derived a formula for the full velocity profile through the urban canopy layer and above (see Fig. 1). It should be noted that the area-averages obtained in these experiments were derived from only five vertical wind profiles and that the inflow wind was perpendicular to the building faces for all cases.

Using data from several wind-tunnel experiments, Kastner-Klein et al. (2002) compared averaged profiles of the longitudinal component of velocity and TKE versus height for several different building configurations. They found for flat-roofed wide building arrays, i.e., essentially 2D flow, that the velocity profiles were nearly linear below building height and had negative values near the ground due to the 2D vortex circulation. For a mock-up of an inner-city area of Nantes, France, measurements from within one street canyon showed the traditional Cionco-Macdonald canopy profile, with reduced velocities in the street canyon and a strong gradient near rooftop.

There have been very few experimental studies in cities that have yielded information on vertical profiles of area-averaged mean wind and turbulence measurements through the depth of the urban canopy. Rotach (1995) obtained vertical profiles of mean wind and turbulence statistics within and above an urban canopy in Zurich, Switzerland by averaging over many days of measurements at a single location. Although not a true area-average, by averaging over many prevailing wind conditions, the single location "samples" different street-level flow conditions (e.g., strong channeling, vortex canyon circulation). The Rotach mean wind profile contains an inflection point, a characteristic feature of many vegetative canopy velocity profiles (e.g., Cionco, 1972). Oikawa and Meng (1997) also measured mean wind and turbulence profiles over many days on a single tower in a suburban area in Sapporo, Japan that were in qualitative agreement with the measurements of Rotach (1995).

Nelson et al. (2004) computed area-averaged profiles of wind speed, TKE, and other turbulence statistics for the reduced-scale Mock Urban Settings Test (MUST) building array. Twenty-four sonic anemometers were located on towers and tripods throughout a 10 x 12 array of shipping containers. Although clearly not representative of a real city, the area-averaged wind speed profiles resembled the vegetative canopy profile with an inflection point at about building height. Results from this experiment will be utilized in this study and more details about the experiment will be given in Section 3 below.

3. EXPERIMENTAL DATA

3.1 Wind-tunnel Experiments.

3.1a. USEPA 7x11 Cubical Building Array.

The experiments were carried out in the U.S. Environmental Protection Agency's meteorological wind tunnel (Snyder, 1979). The "building" array consisted of 7 x 11 cubes (0.15 x 0.15 x 0.15 m) with one H spacing (Fig. 2). The array had a plan area density of 0.25 and a minimum frontal area density of 0.25. The array was immersed in a simulated neutral atmospheric boundary layer created using spires and floor roughness elements. This combination produced a simulated boundary layer with depth of 1.8m, a roughness length of 1mm, and a power-law exponent of 0.16. The inflow wind was perpendicular to the face of the buildings. The Reynolds number based on building height was approximately 30,000, well above the critical value required for Reynolds number independence.

A pulsed-wire anemometer (PWA) was used to measure velocity time series within and around the array at a rate of 10 Hz and an averaging time of 120 seconds. For area-averaging purposes, only measurements within and above the array were used. Below building height, measurements were equally distributed by plan area. A total of 354 measurements were used at each of three heights to obtain area-averaged wind speed below roof-level. Above roof-level between 55 and 85 measurements at each height were used to obtain the area-average, however, there are more measurements above building tops than in street channels.

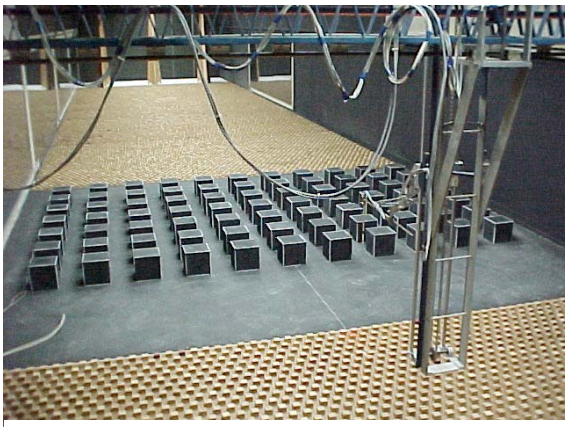

Figure 2. USEPA wind-tunnel interior showing the 7x11 cubical building array. View looking into the wind.

3.1b. Hamburg Oklahoma City Mock-Up.

The experiments took place in the "Wotan" atmospheric boundary-layer wind tunnel at the University of Hamburg in Germany. A wind-tunnel model of the central business district (CBD) of Oklahoma City was constructed at a scale of 1:300 (Fig. 3). An atmospheric boundary layer was established by means of turbulence generators and floor roughness elements. The mean flow profile can be described by a power law with an exponent a = 0.18 and by a logarithmic wind profile with a roughness length z_0 = 0.2 m (full scale). The Reynolds number using an average building height of 50 m (166.7 mm in the wind-tunnel) as reference length scale was approximately 71,000, which is well above the critical value required for Reynolds number independence.

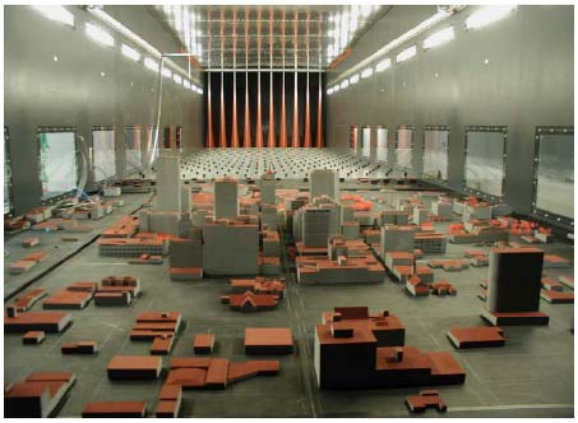

Figure 3. The University of Hamburg wind tunnel showing the model of the Oklahoma City central business district.

High resolution flow measurements were carried out non-intrusively by means of a 2D fiber-optic Laser-Doppler-Anemometer (LDA). The mean and turbulent horizontal velocity components were measured in 4 horizontal planes at z= 10, 20, 40, and 80m (full-scale) in the Park Avenue street canyon and out into the adjacent street intersections (Broadway and Robinson streets). In total, more than 2100 measurement points data were used in the area average calculations. For the case studied here, the wind was from 180°, i.e., perpendicular to the Park Avenue street canyon.

3.2 Outdoor Experiments

3.2a. Mock Urban Settings Test

The DTRA-sponsored Mock Urban Settings Test (MUST) was performed at the US Army Dugway Proving Ground (DPG) in September 2001 (see Biltoft, 2001). MUST consisted of a 10 by 12 aligned array of shipping containers placed in relatively flat terrain surrounded by low shrubbery as seen in Fig. 4. Each shipping container was 12.2 m long, 2.42 m wide, and 2.54 m high (H). The array had a plan area density (λ_p) of 0.10 and frontal area densities (λ_f) of 0.11 and 0.03 using the length and width, respectively (Yee and Biltoft, 2004).

Twenty-four 2D and 3D sonic anemometers were placed around, above, and throughout the array on towers and tripods. Figure 5 shows the relative locations of the instrumentation used in MUST in plan view. The array was aligned approximately 30° west of true north making winds with a bearing of 150° perpendicular to the length of the buildings.

A number of 15 minute periods were analyzed during the night and early morning (8 pm – 3 am) when the prevailing winds were between 60 and 240 degrees. Since the prevailing wind was generally southerly, the area-averaged profiles were produced with a high concentration of sonic anemometers at the leading (southern) edge of the array. The inflow profile was obtained from the 16 m mast on the southern side of the MUST array. Table 1 lists the number of sonics at each height that have been used in this study. The type of sonic anemometer, the organization that operated the

Figure 4. Photograph of the MUST array taken from the southeast corner of the array (courtesy of C.A. Biltoft).

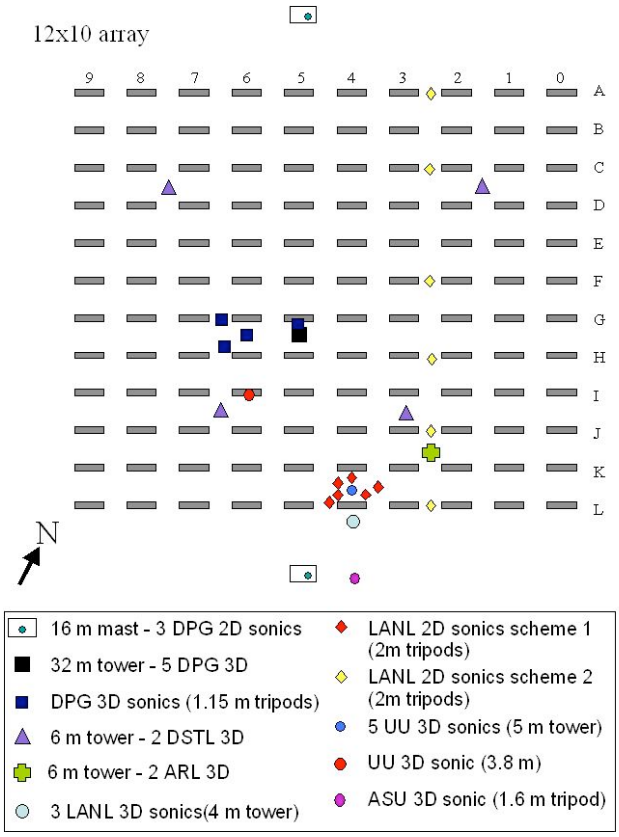

Figure 5. Schematic showing the relative locations of the sonic anemometers employed in MUST. Not to scale. Organizations: ARL (Army Research Laboratory); ASU (Arizona State University); DPG (US Army Dugway Proving Ground); DSTL (Defense Science Technology Laboratory); UU (University of Utah).

sonic anemometer, the relative position of the sonic anemometer, and the sampling frequency for the various sonic anemometers are also given. Note that the canopy height is 2.54 m.

Table 1. MUST instruments for Area Averaging

z(m)	# of Sonics	Organization & Type	Location in Array	SF (Hz)
0.6	1	1 UU 3D	F, z<H	20
1.1	5	1 UU 3D 4 DPG 3D	F,z<H M, z<H	20 10
1.9	6	1 UU 3D 5 LANL 2D	F, z<H F, z<H	20 0.5
2.5	3	1 UU 3D 2 DSTL 3D	F, z~H 1 F/1 B, z~H	20 10
3.9	3	2 UU 3D 1 DPG 3D	1 F/1 M, z>H M, z>H	20 10
6	3	3 DSTL 3D	2 F/1 B, z>H	10
8	1	1DPG 3D	M, z>H	10
16	1	1DPG 3D	M, z>H	10
32	1	1DPG 3D	M, z>H	10

Note: F signifies the front or southern-most rows of the array, M signifies the middle of the array, and B signifies the back or northern-most rows of the array.

3.2a. Joint Urban 2003

The DOE-DTRA-sponsored Joint Urban 2003 field experiment was held in Oklahoma City in July 2003 and involved a large number of collaborating government, university, and commercial sector researchers (Allwine et al., 2004). The goal was to provide information useful for testing and evaluation of the next generation of urban transport and dispersion models. The experiment consisted of a large number of tracer releases, a network of concentration samplers, and fixed meteoro-logical sensors placed in and around the city. About 150 2D and 3D sonic anemometers were placed throughout the city on towers, tripods, lightpoles, building rooftops and other locations and 9 sodars were placed in and around the city.

Figure 6 shows an aerial perspective of the downtown core. Based on the building statistics work of Burian et al. (2005), the average building height in the 500 m x 500 m central downtown core is between 50-70 m with a standard deviation of 40-55 m. The tallest building in the domain is 150 m, while five or six other buildings

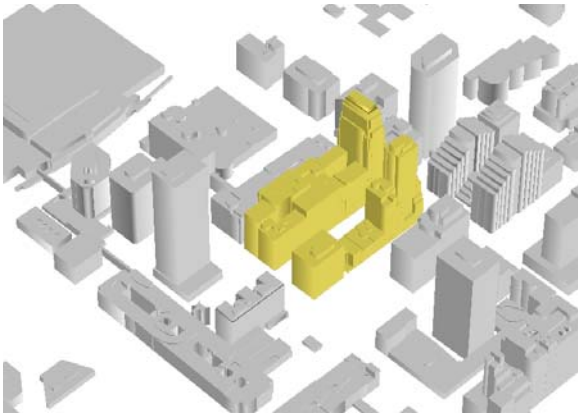

Figure 6. View of the Oklahoma CBD looking from the northeast. The Park Avenue street canyon is highlighted in gold. Building database courtesy of May Yuan, Oklahoma University.

are in the 100 to 120 m range. The downtown core has a plan area density (λ_p) ranging from 0.2 to 0.5 and a frontal area density (λ_f) ranging from 0.25 to 2.0.

Figure 7 shows the relative locations of the instrumentation used for the area averaging. Table 2 lists the number of sonics at each height that have been used in this study, along with the type of sonic anemometer, the organization that operated the sonic anemometer, and the relative position of the sonic anemometer. Note that the inflow winds were most often southerly. For computing area averages, two 30 minute periods were used when the winds were steady and little directional shear occurred with height. The two cases included IOP 3, July 7 at 13:00 LST with prevailing winds of 180 degrees and IOP 5, July 13 at 11:00 LST with winds from 220 degrees.

The instrument distribution below roof-level included 24 anemometers in the east-west running street canyons (e.g., Park Avenue) and 24 anemometers in north-south running street channels (most in intersections, however). At higher elevations, two sodars and one 95 m crane tower were used to obtain area averages. The University of Utah (UU) sodar was placed on the top deck of a parking lot (approx. 20 m agl) on the intersection of N. Broadway and Robert S. Kerr (one block northeast of the Park Avenue street canyon). The ANL sodar was placed at ground level in an open area in the Botanical Gardens about two city blocks south-

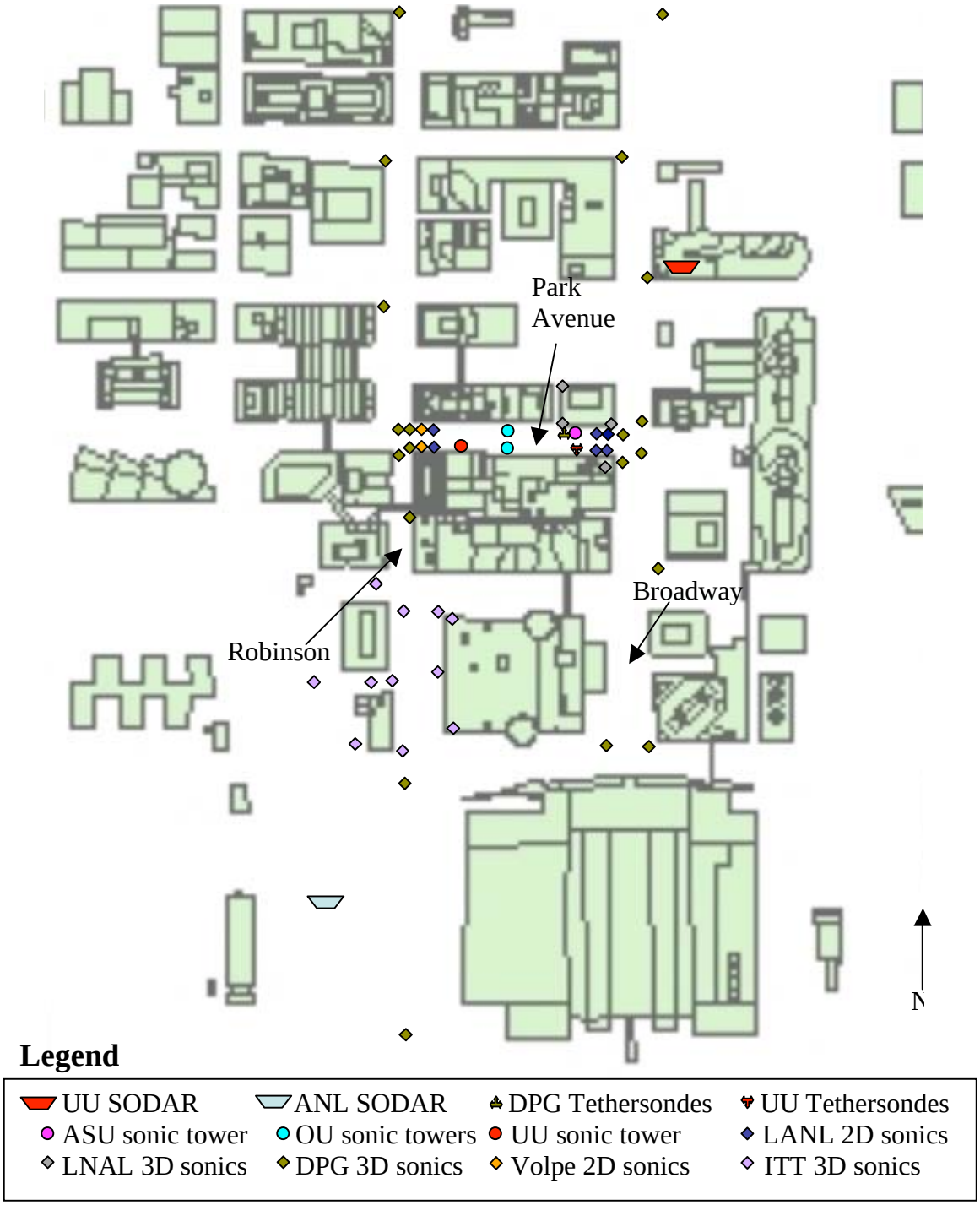

Figure 7. Plan view of downtown Oklahoma City showing the instruments used for deriving the area-averaged urban velocity profile. The LLNL crane tower that supported 3D sonics was located approximately 0.5 miles north of Park Avenue (not shown here).

Table 2. List of instruments used for obtaining the area-averaged urban velocity profile.

Height agl. (m)	Instrument label	Type/Description	IOP3	IOP5
	OU2-1, OU2-2, OU2-3	3D sonics on OU tower 2	X	
1-5 m	OU1-1, OU1-2, OU1-3	3D sonics on OU tower 1		X
	DPGth6	DPG Tethersonde	X	
Total no. of	UUth6, UUth5	UU Tethersonde	X	X
measurements=26	ASU3, ASU2	3D sonics on ASU tower	X	X
	Handar-black, green	2D sonics on tripod	X	X
	Handar-red, white, yellow	2D sonics on tripod	X	X
	Metek-white	3D sonic on tripod	X	X
	UU03, UU05, UU08	3D sonics on UU tower	X	X
	ITT02, ITT04-ITT10	3D sonics on tripod	X	X
	DPGth5	DPG Tethersonde	X	X
	UU10, UU11	3D sonics on UU tower	X	X
7-10 m	ASU1	3D sonic on ASU tower	X	X
	DPG01- DPG20	3D sonics on street lights	X	X
Total no. of	LLNL-A	3D sonic on crane tower	X	X
measurements=27	OU2-4	3D sonic on OU tower 2	X	
	OU1-4	3D sonic on OU tower 1		X
	DPGth4	DPG Tethersonde	X	X
	UUth4	UU Tethersonde	X	X
	OU2-5	3D sonic on OU tower 2	X	
16-20 m	OU2-5	3D sonic on OU tower 1		X
	ITT03, ITT07	3D sonics on building roof tripod	X	X
Total no. of	LLNL-B, LLNL-C	3D sonics on crane tower	X	X
measurements=7	DPGth3	DPG Tethersonde	X	X
	UUth3	UU Tethersonde	X	X
30 m	DPGth2	DPG Tethersonde	X	X
	UUth2	UU Tethersonde	X	X
Total no. of	LLNL-D	3D sonic on crane tower	X	X
measurements=3				
	DPGth1	DPG Tethersonde	X	X
40-55 m	Metek-yellow, black	3D sonics on side of building	X	X
	Metek-blue, green	3D sonics on side of building	X	X
Total no. of	LLNL-E, LLNL-F	3D sonics on crane tower	X	X
measurements=8	Metek-red	3D sonic mounted on rooftop	X	X
	ANL SODAR	Botanical Garden SODAR	X	X
	UU SODAR	Parking Garage SODAR	X	X
60-75 m	LLNL-G	3D sonic mounted on a crane tower	X	X
Total no. of	ANL SODAR	Botanical Garden SODAR	X	X
measurements=9	UU SODAR	Parking Lot SODAR	X	X
75-95 m	LLNL-H	3D sonic mounted on a crane tower	X	X
Total no. of	ANL SODAR	Botanical Garden SODAR	X	
measurements=9	UU SODAR	Parking Garage SODAR	X	
95-105 m	ANL SODAR	Botanical Garden SODAR	X	
Total no. of	UU SODAR	Parking Garage SODAR	X	
measurements=8				
105-125 m	ANL SODAR	Botanical Garden SODAR	X	
Total no. of measurements=2				

west of the Park Avenue street canyon. The 95 m crane tower was about 1 km north of Park Avenue and located to the north of several tall buildings.

The "inflow" profile was obtained using the PNNL sodar, located about 2 kilometers to the SSW of the central business district, and a rooftop prop-van anemometer at 55 m agl (and 25 m above roof level), located about 1 km directly south of the downtown core. It will be shown later that the sodar wind speed at 55 m agl was often in disagreement with the rooftop anemometer, but since the rooftop anemometer was much closer to and immediately south of the downtown core it is felt that this measurement better represents the inflow profile.

4.0 COMPUTATIONAL FLUID DYNAMICS MODEL DESCRIPTIONS

Two computational fluid dynamics (CFD) codes and one diagnostic-empirical fluids code were used in this study to compute area-averaged wind speed profiles in cities. CFD-URBAN and FLUENT-EPA both solve the Reynolds-Averaged Navier-Stokes (RANS) equations and use a one-and-a-half order two-equation k-ε turbulence closure scheme. QUIC uses empirical parameterizations to define building-induced flow circulations and then imposes mass conservation. More details on CFD-URBAN, FLUENT-EPA, and QUIC can be found in Coirier et al. (2005), Huber et al. (2005), and Pardyjak and Brown (2001), respectively.

The CFD-URBAN code was used to compute flow fields for downtown Oklahoma City on a 1.25 km by 1.25 km domain (Coirier and Reich, 2003). Grid size was close to 1 meter near buildings and expanded outwards. The domain included 3.8 million cells made up of prismatic and hexahedral elements. Outside of the urban core, building volumes were represented as drag elements. FLUENT-EPA was used to simulate a 2 km by 2 km area of Manhattan centered on the Madison Square Garden arena (Huber et al., 2006). Grid size was 2 meters near buildings and expanded outwards. The domain included 19 million cells made up of mostly hexahedral, pyramidal, and tetrahedral elements. QUIC was used to compute flow fields in a 5x5 block region of downtown Salt Lake City (Gowardhan et al., 2006). The domain was 1.2 x 1.1 km and included 2 million grid cells at 5 m resolution. In all three cases, neutral stability was assumed and steady-state inflow winds were applied.

5.0 AREA-AVERAGING METHODOLOGY

To obtain the area-average wind speed as a function of height, we take the time-averaged U and V components of velocity for each instrument (or measurement point), and then take the average U and V across all instruments (or measurement points) at the same height (or within a height bin). We then use these area-averaged U and V velocities to obtain the area-averaged wind speed at a particular height. The measurements should be uniformly distributed horizontally, so as not to bias the answer, but for outdoor field experiments this is seldom the case (for example, see Figs. 5 and 7). One of the potential advantages of using computational fluid dynamics models to obtain area-averages, and in some cases wind-tunnel experiments, is the high density and spatial coverage of data they provide.

The vector area average approach is used instead of the scalar area average (i.e., taking the average of all the wind speeds measured by each instrument) because we are interested in obtaining the net transport velocity for plume transport and dispersion calculations. For example, if wind measurements were taken at points in a horizontally-rotating vortex, the scalar-averaged wind speed would be large. But, a tracer released into the vortex would travel in a circle, with no net transport, in agreement with the vector-averaged wind speed.

The area-average wind speed can be computed accounting for the area (or volume) occupied by buildings (i.e., accounting for the “zero” wind speeds inside buildings) or by only considering the area outside of buildings (i.e., the air volume). Figure 8 shows the area-averaged wind speed computed for the wind tunnel 7x11 cube array using the entire horizontal plane in one case (pink profile) and using only the grid cells that are outside of buildings in the other case (red profile). Since the plan area density is 25% for this case, the winds are 25% smaller when including the “zero” wind speeds from inside the buildings.

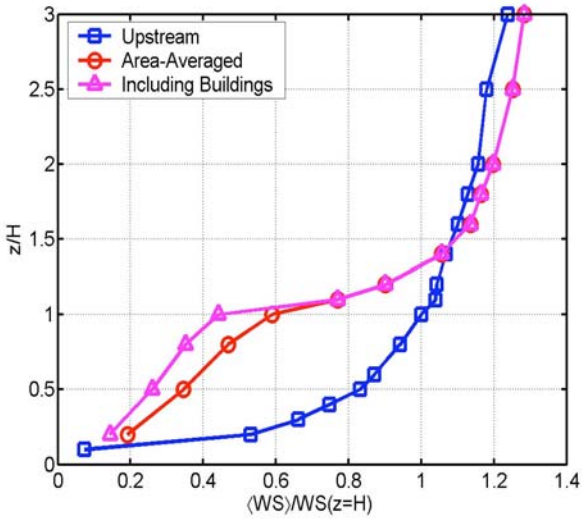

Figure 8. Area-averaged wind speed profile versus height for the 7x11 cubical building array showing the effect of the averaging area. The pink profile was created by averaging over the entire horizontal area and includes the "zero" velocities where buildings are located; the red profile was computed by averaging over only part of the horizontal area, only where buildings are not located. Inflow winds perpendicular to the building face. $\lambda_f = \lambda_p = 0.25$, $\sigma_h = 0$ m.

What type of result is needed depends on the application and how a particular model treats mass conservation. A few mesoscale models have developed urban canopy schemes, for example, that include the volume lost to (the sub-grid scale) buildings in the mass conservation equation (e.g., Ca et al., 1999). Most mesoscale models, however, treat the buildings as volumeless drag elements. In the former case, including the building area in the area averages is most appropriate; in the latter case, ignoring the building area is most correct.

In the downtown areas of large cities, this difference in how the vector average is calculated leads to a significantly different answer. The plan area density in a downtown area can easily surpass 0.5, which means that more than half the area is covered by buildings and that the area-averaged wind speed accounting for building volume is 50% smaller than when computed the other way. In this paper, for simplicity, we compute only the area-averaged wind speed in the air volume, excluding the zero values within buildings.

There are some ambiguities that develop when reporting area-averaged wind speed for problems that approach two dimensionality (e.g., arrays of very wide buildings) since there is backflow on average near the ground, i.e., for these cases the area-averaged wind direction should be reported too. One could also report the area-averaged U component, but since for real-world problems the flow is three dimensional and the inflow wind is seldom perpendicular to building faces, it becomes difficult to simultaneously interpret the area-averaged U and V components.

6. EXPERIMENTAL MEASUREMENTS

The area-averaged wind speed profile computed for the 7x11 cubical building array with $\lambda_f = 0.25$ is very similar to that measured by MacDonald (2000) for the aligned cubical building array with a similar frontal area density (compare Figs. 1 and 8). This result suggests that the limited number of measurements (5 vertical profiles only) used by MacDonald was adequate for representing the area average velocity in the cubical array.

Figure 9 shows the area-averaged wind speed profile for Park Avenue measured in the Hamburg wind tunnel. Although the experimental domain included most of the greater downtown area, the measurements used for the area-average computations were from within Park Avenue and the adjacent street intersections only. The plan area density in the immediate vicinity of Park Avenue is approximately 0.4 and the frontal area density for a southerly inflow is approximately 2.0. The majority of buildings defining the street canyon were approximately 50 m high, but buildings ranged from 10 m to 120 m (full-scale).

Although the Park Avenue area is high density ($\lambda_f = 2.0$), the Park Avenue area-averaged profile lies closest to the Macdonald measurements for $\lambda_f = 0.2$. Several explanations could account for the disparity. First, the results of Macdonald may be specific to cubical building arrays and not extrapolate to wider building arrays where the flow becomes more two-dimensional. Macdonald (2000) did find different results for staggered non-aligned cubical arrays, for example. A second possible

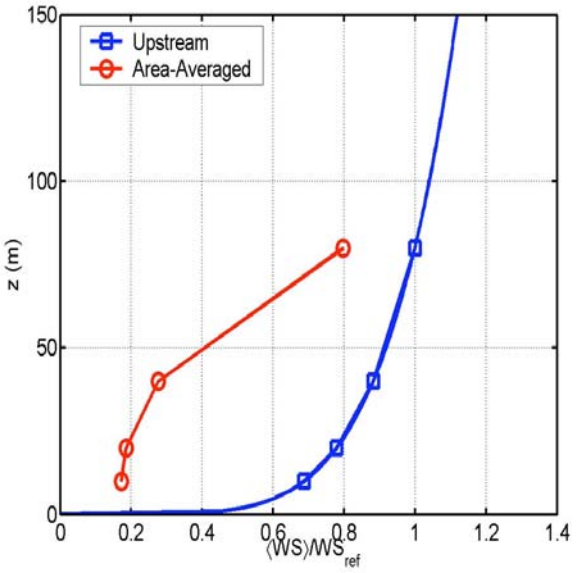

Figure 9. The area-averaged wind speed profile (red) and the upstream inflow profile (blue) for the Park Avenue wind-tunnel experiment. Inflow winds are perpendicular to the Park Avenue axis. λ_f = 2.0 (WD = 180°), λ_p = 0.4, average height = 65 m, σ_h = 50 m (full-scale).

explanation could be that the Park Avenue results are for a non-idealized street canyon, whereas the Macdonald results are for an idealized building array. In Park Avenue, the buildings vary with height, such that in portions of the canyon reverse flow will extend up to different heights, and where the buildings are low there may be strong inflow or outflow just above the local rooftop resulting in strong winds below the average building height. Hence, the area-averaged profile in a real city may actually be better represented by averaging together different Macdonald-Cionco profiles created from a distribution of building heights. Note that the area-averaged profiles of wind speed and the U component of velocity for the Park Avenue experiment fall nearly on top of one another, thus the difference with the Macdonald results are not due to the fact that MacDonald reported the area-average U component of velocity and we are reporting area-averaged wind speed.

In comparing the 7x11 building array and the Park Avenue wind-tunnel experiments both show a strong reduction in the area-averaged wind speed below building height (Figs. 8 and 9). At z/H=1/2, the wind speed is reduced nearly 60% from upstream speeds for the 7x11 array case and nearly 75% for the Park Avenue street canyon. The area-averaged wind speed returns to ambient values at about 1.4 H for the 7x11 cube array. Extrapolating for the Park Avenue case, the height where the wind speed deficit disappears is about 1.5 H (dependent, of course, on how one extrapolates). However, note that the tallest buildings on the street go up to 120 m. Also, note that the height to which the velocity deficit occurs is dependent on the upwind fetch of the building array. For the wind-tunnel 7x11 array, the measurements begin at the upstream edge of the array, while the Park Avenue measurements are well north. The height at which the area-averaged wind equals the upstream wind will be lower compared to further downstream where the internal boundary layer has had a chance to grow and is deeper.

On average, area-averaged wind profiles from the MUST shipping container array show much smaller wind speed deficits below building height (Fig. 10). This is expected given the small frontal area density ($\lambda_{f,\,max}$ = 0.11) of the array. However, when looking at the plots colored by wind direction, one can see that for winds near 150 degrees (perpendicular to the wide face of the shipping containers) the area-averaged wind speed is significantly reduced. The larger area-averaged wind speeds found below building height occur when the inflow wind is oblique to the long face of the shipping containers and hence probably represents cases when channeling is present. The smaller wind speed deficits for lighter inflow winds (see Fig. 10b) may result because of the relatively larger wind direction fluctuations that occur under light wind conditions and hence steady recirculating vortices are less likely to consistently appear.

Area-averaged wind speed profiles for downtown Oklahoma City are plotted for inflow aligned with the street array (Fig. 11) and at oblique angles to the street array (Fig. 12). Figure 11 shows that when the winds are from the south, there is significant reduction in the area-averaged wind speed due to the downtown buildings. At 50 m, there is a 70 to 80% reduction in wind speed relative to the inflow wind. When the inflow winds are more from the west, the reduction in area-averaged wind speed is considerably smaller (Fig. 12). This may be

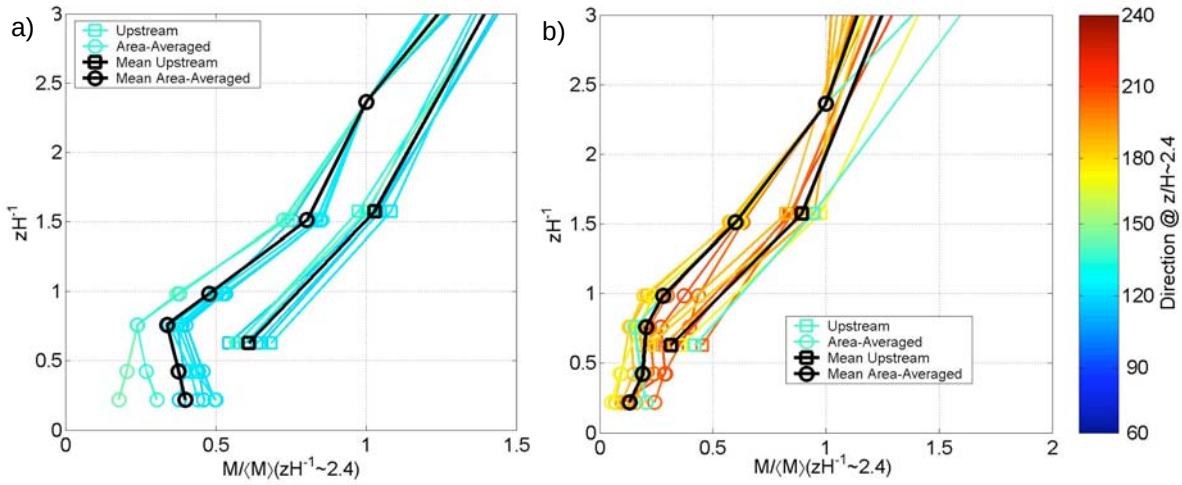

Figure 10. Ensemble-averaged area-average wind speed profile (black, circles) and the ensemble upstream "inflow" profile (black, squares) for the MUST shipping container array for a) strong inflow winds (>4 m/s at z/H = 6.3) and b) light inflow winds. Also shown are individual 15 minute average profiles colored by inflow wind direction (150° is perpendicular to the long face of the buildings). λ_f = 0.11 (WD° = 150) and λ_f = 0.03 (WD = 240° and 60°), λ_p = 0.10, σ_h = 0 m.

due to several reasons. First, the effective frontal area density is smaller for westerly winds (the blocks are shorter in the north-south direction) and thus the wind speed reduction is expected to be smaller. A second reason may be due to the finite number of measurement locations, and for westerly winds a larger fraction of the instruments are in east-west running street channels versus in sheltered north-south running street canyons, thus biasing the area-average computations. Finally, note that there is considerable uncertainty regarding the inflow profile due to lack of nearby upwind measurements near ground level, the distance of the sodar from the downtown area, and uncertainty in the lowest measurements from a sodar. The effect of the downtown buildings on the area-averaged profile is difficult to quantify due to the uncertainty in the undisturbed upwind profile.

7. "SYNTHETIC" DATA

High resolution CFD calculations were performed for regions of New York City and Oklahoma City providing millions of points over which to obtain area averages. A lower resolution diagnostic-empirical fluids model was used to perform simulations in downtown Salt Lake City and provided a 3D wind field which contained over a million data points to use for area-averaging. Data from the periphery of the domains were not used in the area-averaging. The NYC Manhattan domain is centered on the Madison Square Garden sports arena and is a relatively dense area with little open space. The λ_p = 0.6, λ_f = 1.3 -1.6, average building height = 93 m, and σ_h = 41 m (Burian et al., 2005b). The Oklahoma City domain has a dense core, but also low squat buildings on the southern side and numerous outdoor parking lots. The northern side has λ_f = 1.5, average building height = 65 m, and σ_h = 50 m (Burian et al., 2005a). The southern side has λ_f = 0.4, average building height = 27 m, and σ_h = 23 m. The average λ_p is about 0.4 over the entire area. Salt Lake City is closer to Oklahoma City in size and density, however, the domain only includes the smaller hi-rise buildings on the southern side of the downtown area. The λ_p = 0.25, λ_f = 0.18 (for a southerly wind direction), the average building height = 23 m, σ_h = 20 m, and the majority of buildings were between 5 and 100 m high (Burian et al., 2005c).

Figure 13 shows the New York City area-averaged wind speed profile for several inflow wind directions. The profile resembles the Cionco-Macdonald profiles for very large λ_f, except that there is not the sharp gradient where

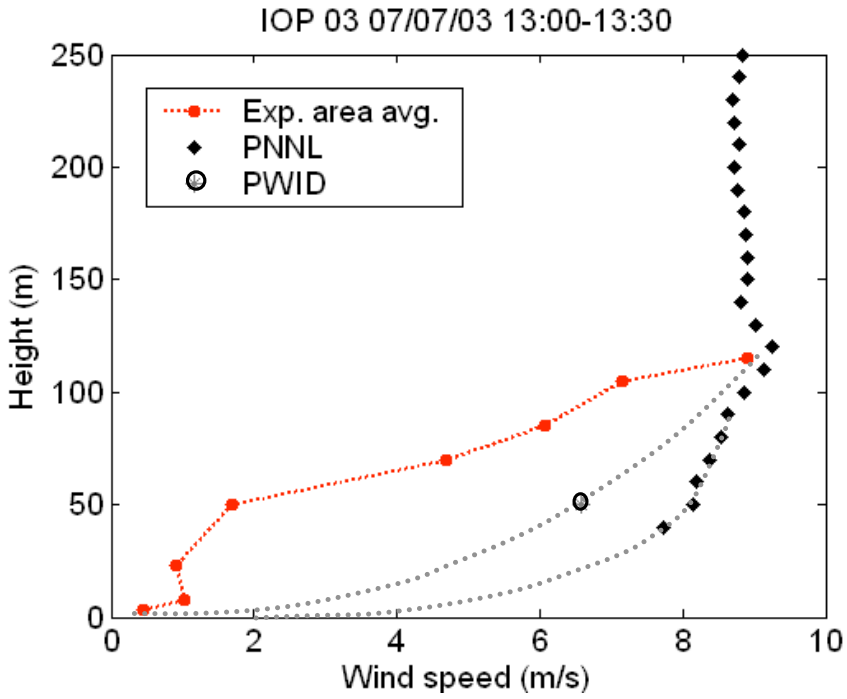

Figure 11. Area-averaged wind speed profile (red) for downtown Oklahoma City with upwind measurements (black symbols). Inflow wind direction between 180 – 190°. For the southern and northern halves of the domain: avg. building height = 27 & 65 m, λ_f = 0.5 & 1.6 (WD° = 180) , λ_p = 0.4 & 0.4, σ_h = 23 & 50 m, respectively.

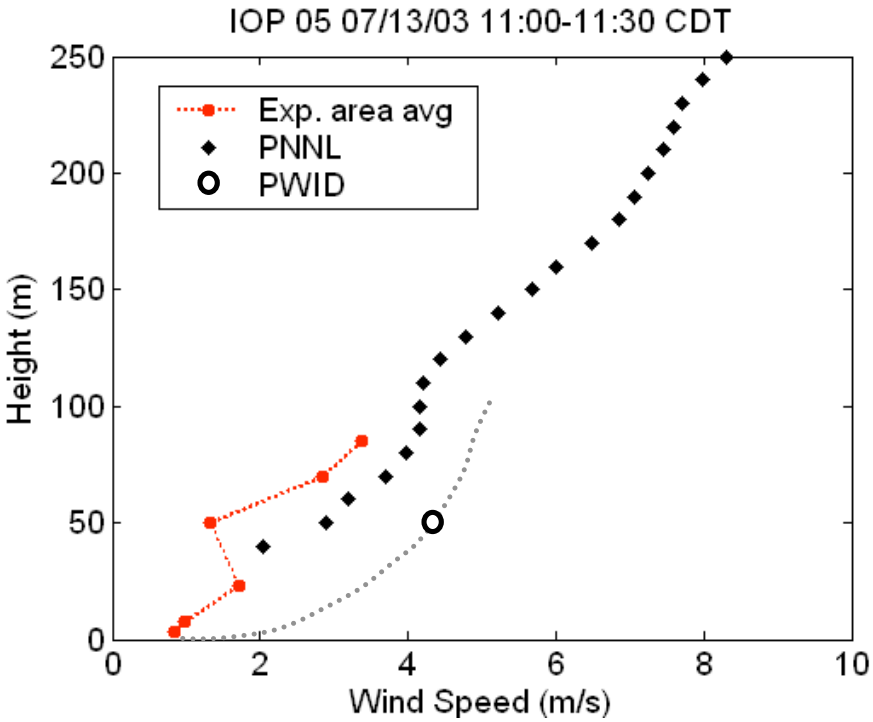

Figure 12. Area-averaged wind speed profile (red) for downtown Oklahoma City with upwind measurements (black symbols). Inflow wind direction of 250°.

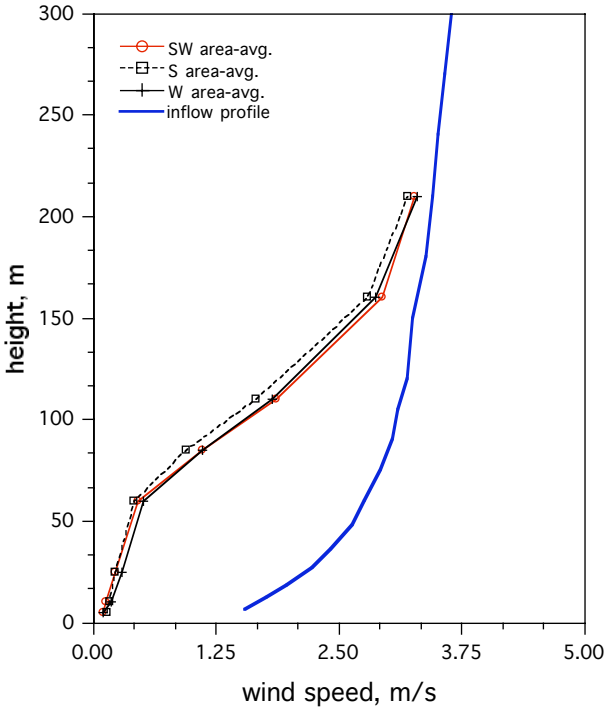

Figure 13. Area-averaged wind speed for Manhattan obtained using the FLUENT-EPA CFD model. Profiles were computed for three different inflow wind directions (S, SW, and W). Average building height = 93 m, σ_h = 41 m, λ_f = 1.3 - 1.6, λ_p = 0.6.

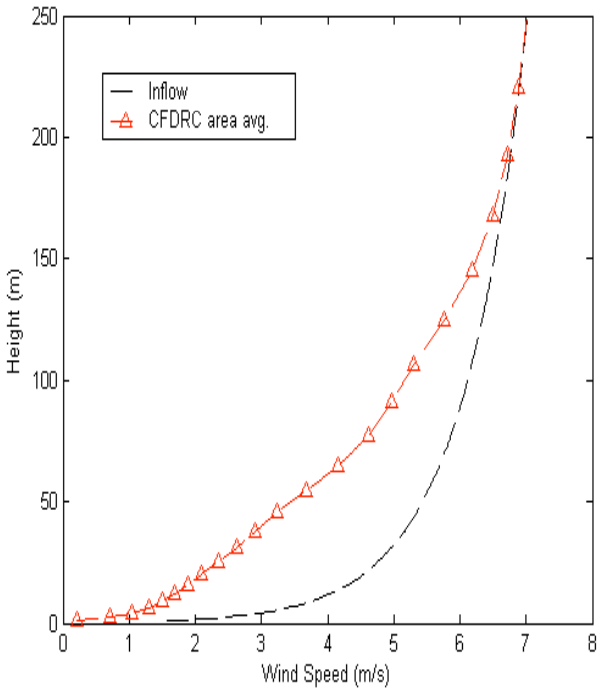

Figure 14. Area-averaged wind speed for downtown Oklahoma City obtained using the CFD-URBAN model. Profiles were computed for a southerly inflow wind direction. For the southern and northern half of the domain, respectively: average building height = 27 & 65 m, σ_h = 23 & 50 m, λ_f = 0.5 & 1.5, λ_p = 0.4 & 0.4.

the wind speeds at rooftop. As mentioned earlier, this is most likely due to the fact that there is no one building height, and that instead there are many heights at which winds locally speed up and on average they result in the observed profile. Also shown in Figure 13 are area-averaged wind speeds for a southerly, southwesterly, and westerly inflow direction. There is little visible difference in the resulting area-averages velocity profiles.

Figures 14 shows the Oklahoma City area-averaged wind speed profile for a southerly inflow wind direction. The profile shows that the city has much less effect on the area-averaged wind speed compared to New York City. In fact, when comparing to the area-averaged measurements from Oklahoma City (Fig. 11), the model appears to underestimate the reduction in wind speed. However, it may also point out the bias of our instrument layout, where more wind instruments are placed in dense built-up areas (i.e., more “interesting” areas where the flow varies a lot spatially) than in more open areas (i.e., less “interesting” areas because the winds may be more homogeneous spatially). This is supported by the fact that the wind-tunnel measurements obtained in Park Avenue, a built-up area of Oklahoma City, agree more or less with the field measurements from the greater downtown area. A more careful evaluation and comparison of the CFD results should be done with the experimental data through a point-by-point comparison.

Figure 15 shows the Salt Lake City area-averaged wind speed profile for a southerly inflow direction. This profile is similar to the area-averaged Oklahoma City profile. Although the influence of the city appears to not be as significant in relation to other cases, one should note that at z = 10 m, there is approximately a 50% reduction in wind speed as compared to the inflow wind speed. These results were obtained with an approximated fluids code and therefore

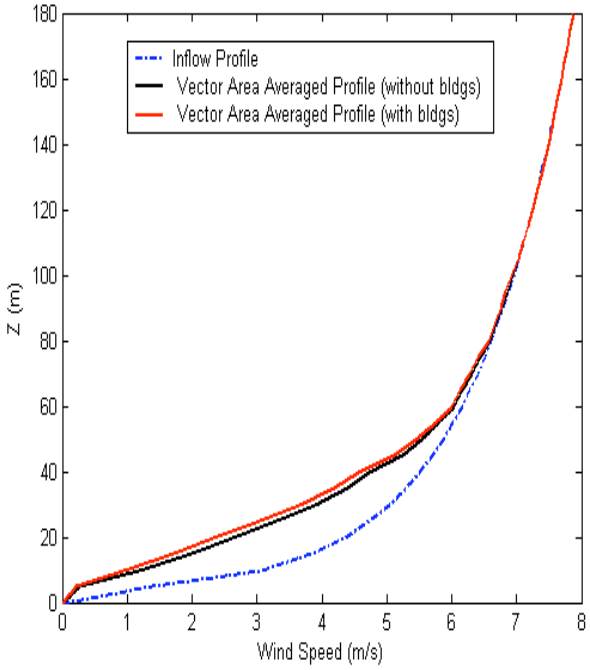

Figure 15. Area-averaged wind speed for downtown Salt Lake City obtained using the QUIC model. Profiles were computed for a southerly inflow direction. Average building height = 23 m, σ_h = 20 m, λ_f = 0.18, λ_p = 0.25.

to gain confidence in the results further comparisons to experimental data and CFD output is necessary. Note that an area-averaged profile is also shown that was computed using the area occupied by buildings.

7. SUMMARY

In this paper, we have derived area-averaged wind speed profiles for idealized and complex building configurations. Area average profiles were derived from laboratory experimental data, full-scale experimental data, and from computational fluid dynamics models. The results suggest that the Cionco-Macdonald canopy profiles do a good job of describing the profiles, though some modifications may need to be made for cities of high density and variable building height. These data should be useful for evaluating the new generation of mesoscale models with urban canopy parameterizations.

8. REFERENCES

Allwine K.J., M. J. Leach, L. W. Stockham, J. S. Shinn, R. P. Hosker, J. F. Bowers, and J. C. Pace: Overview of Joint Urban 2003, 2004: An atmospheric dispersion study in Oklahoma City, AMS Symp. on Planning, Nowcasting, & Forecasting in the Urban Zone, Seattle, WA.

Brown, M., 2001: Urban parameterizations for mesoscale models, in Mesoscale Atmospheric Dispersion, pp. 193-255, Z. Boybeyi, ed., WIT Press, Southampton, UK. LA-UR-99-5329.

Brown M. and M. Williams, 1998: An urban canopy parameterization for mesoscale meteorological models, 2nd AMS Urb. Env. Symp., Albuquerque, NM, LA-UR-98-3831.

Burian, S., A. McKinnon, J. Hartman, W. Han, 2005: National Building Statistics Database: Oklahoma City, LA-UR-05-8153, 17 pp.

Ca V., Asaeda, T., & Ashie, Y., 1999: Development of a numerical model for the evaluation of the urban thermal environment, *J. Wind Eng. Ind. Aerodyn.*, **81**, pp. 181-196.

Chin, H.-N. S. , M. Leach, G. Sugiyama, J. Leone Jr., H. Walker, J. Nasstrom, and M. Brown, 2005: Evaluation of an urban canopy parameterization in a mesoscale model using VTMX and URBAN 2000, Mon. Wea. Rev., **133**, pp. 2043-2068.

Cionco, R., 1972: A wind-profile index for canopy flow, *Bound.-Layer Meteor.*, **3**, pp. 255-263.

Coirier, W.J., Fricker, D.M, Furmanczyk, M., and Kim, S., 2005: A Computational Fluid Dynamics Approach for Urban Area Transport and Dispersion Modeling, Environmental Fluid Mechanics, in print.

Coirier, W.J. and A.J. Reich, 2003: Oklahoma City high-resolution dispersion simulation, CFDRC Final Report, 23 pp.

Gowardhan, A., M. Brown, M. Williams and E. Pardyjak, 2006: Evaluation of the QUIC Urban Dispersion Model using the Salt Lake City

URBAN 2000 Tracer Experiment Data – IOP 10, 6th AMS Urban Env. Conf., Atlanta, GA.

Holt, T. and J. Shi, 2004: Mesoscale simulations of the urban environment of Washington D.C.: Comparison of COAMPS simulations to DCNET observations and sensitivity of plume transport to an urban canopy parameterization, AMS Symposium on Planning, Nowcasting, and Forecasting in the Urban Zone, Seattle, WA.

Huber, A., M. Freeman, R. Spencer, B. Bell, K. Kuehlert, and W. Schwarz, 2006: Development and Application of CFD Simulations Supporting Urban Air Quality and Homeland Security, 6th AMS Urban Env. Conf., Atlanta, GA.

Huber, A., W. Tang, A. Flowe, B. Bell, K. Kuehlert, and W. Schwarz, 2005: Development and applications of CFD simulations in support of air quality studies involving buildings, 13th AMS Conf. on Air Poll. Meteor., Vancouver, BC.

Kastner-Klein, P., M. W. Rotach, M. J. Brown, E. Fedorovich and R. E. Lawson, 2000: Spatial Variability of Mean Flow and Turbulence Fields in Street Canyons, 3rd AMS Urban Env. Symp., Davis, CA. LA-UR-00-3025.

Martilli, A., A. Clappier, M. Rotach, 2002: An urban surface exchange parameterisation for mesoscale models, *Bound.-Layer Meteor.*, **104**, pp. 261-304.

Masson, V., 2005: Urban surface modeling and the meso-scale impact of cities*, Theoretical & Applied Climatology*, v 5-6.

Nelson, M., M. Brown, E.R. Pardyjak, J. Klewicki, 2003: Area-averaged profiles over the Mock Urban Setting Test array, AMS Conf. on Urban Zone, Seattle, WA, LA-UR-0452-78, 5 pp.

Oikawa, S. & Meng, Y., 1997: A field study of diffusion around a model cube in a suburban area, *Bound.-Layer Meteor.*, **84**, pp. 399-410.

Otte, T., A. Lacser, S. Dupont, and J. Ching, 2004: Implementation of an urban canopy parameterization in a mesoscale meteorological model, J. Appl. Meteor., **43**, pp. 1648-1665.

Pardyjak, E. and M. Brown, 2001: Evaluation of a fast-response urban wind model – comparison to single-building wind-tunnel data, Int. Soc. Environ. Hydraulics, Tempe, AZ, LA-UR-01-4028, 6 pp.

Rotach, M., 1995: Profiles of turbulence statistics in and above and urban street canyon, *Atmos. Env.*, **29**, pp. 1473-1486.

Snyder, W., 1979: The EPA Meteorological Wind Tunnel: Its Design, Construction, and Operating Characteristics. Rpt. No. EPA-600/4-79-051, Envir. Prot. Agcy., Res. Tri. Pk., NC, 78p.

Sorbjan, Z. & M. Uliasz, 1982: Some numerical urban boundary-layer studies, *Bound.-Layer Meteor.*, **22**, pp. 481-502.

Urano, A., Ichinose, T., & Hanaki, K., 1999: Thermal environment simulation for three dimensional replacement of urban activity, *J.Wind. Eng. Ind. Aerodyn.*, **81**, pp. 197-210.

Yee, E., and Biltoft, C. A., 2004: Concentration fluctuation measurements in a plume dispersing through a rugular array of obstacles. Bound. Layer Meteor., **111**, pp. 363-415.